

**TKI 2022**

## Comparison of the Stiffness of 3D-Printed Wire Raceway Slewing Bearing Based on Simplified FEA Model and Experiment

Dominik GUNIA\*<sup>ORCID</sup>, Tadeusz SMOLNICKI<sup>ORCID</sup>, Mariusz STAŃCO

*Wroclaw University of Science and Technology*

Wroclaw, Poland; e-mails: tadeusz.smolnicki@pwr.edu.pl, mariusz.stanco@pwr.edu.pl

\*Corresponding Author e-mail: dominik.gunia@pwr.edu.pl

The wire-raceway bearings are a subcategory of slewing bearings. Their popularity has recently increased due to their advantages, including weight that is lower than that of other similar slewing bearings, and the ability of transferring various loads, such as axial load, radial load and tilting moment. Currently, metal rings (steel or aluminum) are the most popular choice for all kinds of slewing bearings; however, with advent of additive manufacturing a new ‘chapter’ opens for the development of wire raceway slewing bearings, where the interface between the rolling elements and the raceway is the same as in other bearings (i.e., contact between steel-steel). At the same time, rings can be made from other lightweight materials, such as composites or plastics, with high-level shape customization due to 3D printing. Stress between wire raceways and rings is much lower. Hence, rings’ lower material properties do not significantly affect bearing capacity. Proper calculation methodology should be created to analyze lightweight wire raceway bearings, as materials can differ significantly from typical materials covered by current theories. The paper presents a prototyped 3D-printed bearing with rings made from polylactic acid (PLA). The bearing stiffness is measured and compared with the simplified finite element analysis (FEA) model using the equivalent bearing model with nonlinear springs and beam elements.

**Keywords:** wire raceway bearings; slewing bearings; bearing stiffness; 3D printing.

### 1. INTRODUCTION

This paper aims to analyze the stiffness of wire raceway bearing with 3D-printed rings. 3D printing allows for the easy manufacturing of complex shapes without machining. PLA was used as ring material, which reduced bearing weight. Wire raceways and balls were sourced from a market set of 4-point wire raceway bearing components [1]. The main advantage of wire raceway bearings is their lower mass compared to standard slewing bearings. Therefore, this parameter

is crucial and it is worth focusing on for further reduction. The main industries using wire raceway bearings are aerospace, robotics, and medical devices. In all applications, weight is very important. However, from a load point of view, forces acting on components can differ significantly between aerospace and robotics. Aerospace applications may demand higher forces, while in some robotic applications, force requirements are much lower, and primary focus is on reducing the weight and inertia of the robot itself, which can be achieved through the mass reduction of components.

A common configuration in wire raceway bearings involves combining steel raceways with rings made from materials possessing lower properties. However, the use of 3D printing and plastic rings in wire raceway bearings is less common. Such an approach allows for reducing the weight of the bearing and also simplifies the manufacturing process, as all machines can be replaced by a single 3D printer. Moreover, rings shape can be adjusted to meet the structure needs, for example, to higher stiffness in some areas. A section view of a typical, 4-point wire raceway bearing is presented in Fig. 1. Additive manufacturing also allows to print with carbon fibers, both short and continues, which leads to a further increase in material strength of resulting composite material components.

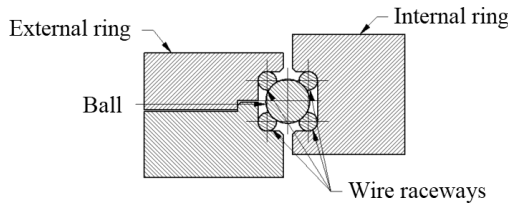


FIG. 1. The section view of the wire raceway bearing.

Literature regarding slewing bearings is extensive and covers several analyses of various bearing types and designs. Calculating the slewing bearing capacity using FEA and creating simplified equivalent models of slewing bearings by using nonlinear springs were developed by multiple authors [2–5, 7]. Another important topic covered by studies is fatigue life assessment of slewing bearings. As raceways are hardened, crack propagation is different in each layer, with the lowest ratio in the core layer [6]. Another factor affecting large-diameter slewing bearings is a gap between rolling elements and raceways, which can affect fatigue life [7, 8]. The presence of gaps in large-diameter slewing bearings can result from the manufacturing process. Slewing bearings show various wear mechanisms depending on the heat treatment of the raceway. In the raceway with low hardness, it is very likely that the plastic flow of material will occur, which can affect initial bearing geometry and lead to the development of a secondary raceway [9].

Another topic covered in the literature regarding large-diameter slewing bearings is improvements in the design. One of the potential methods of reducing stress in the raceway is modifying its shape by introducing correction, which helps avoid damage on the raceway edge [10].

Even though there are various proposed models for replacing rolling elements in slewing bearings, new methods are emerging to improve current FEA models by adding more spring elements or creating more analytical approaches [11, 12].

However, there is still very little information about the wire raceway bearings. Current papers are focused mainly on the development of analytical methodology of calculation and including additional phenomena related to wire raceways, such as wire twisting [13–15]. The only presented model of the simplified FEA model of wire raceway bearing was focused on analytically calculated stiffness of rollers and wire, and it was implemented into FEA by built-in feature [16]. That approach was successful in a limited range of loads.

Previous stress distribution analysis showed that the highest stress is in contact pair *ball-wire raceway*, while in contact pair *wire-ring* stress is much lower. Hence, materials with lower properties can be used [17]. In order to check the boundaries of wire raceway bearings, real results, such as bearing capacity and stiffness, are necessary. Moreover, it is interesting to know what materials can be used for rings to further reduce weight. A prototyped 3D-printed bearing was created with PLA rings. However, the main question was whether PLA can carry a load and how it affects bearing stiffness. It is worth mentioning that 3D printing allows using various materials, such as plastics, reinforced plastics and metals. In that particular case, PLA was chosen for its popularity and ease of printing, and not for its specific properties.

In order to create an equivalent FEA model, a special approach is needed, as the additional contact pairs in wire bearing increase the problem difficulty. Due to nonlinear contacts, the conventional approach can lead to time-consuming analysis with problematic convergence. To avoid these issues, an equivalent model was developed, where balls and wire raceways were replaced by a combination of nonlinear springs and beam elements. Such an approach allows to simulate the entire bearing in a short time. Additionally, factors such as bearing clearance/preload or structure stiffness can be included.

## 2. METHODOLOGY

As mentioned, bearing rings were 3D printed, while the remaining components (balls and wire raceways) were obtained from a market bearing set. Bearing geometric parameters are presented in Table 1. Wire raceways can have various customized shapes, and in this particular case, wire raceways with circular sections were used. The osculation factor is equal to 0.96. According to the

**Table 1.** Bearing geometric properties.

Bearing diameter $\phi$ [mm]	Number of rolling elements $n$	Ball diameter $d$ [mm]	Wire diameter $\lambda$ [mm]	Osculation ratio $s$
200	42	9.525	4	0.96

manufacturer, wire raceways were made from spring steel (54SiCr6), and the balls were made from 100Cr6 steel.

In order to verify the prototype, axial stiffness was measured. Moreover, an equivalent FEA model was developed and its results were compared with the test results. The prototype bearing with 3D printed rings is presented in Fig. 2. Weight of the prototype bearing is equal to 1.4 kg, while that of the bearing with aluminum rings is equal to 2.4 kg.

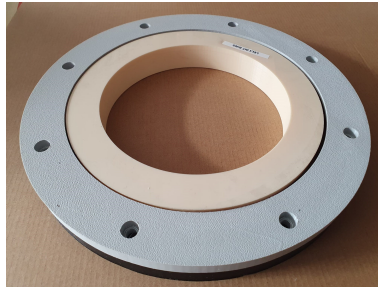


FIG. 2. 3D-printed rings of wire raceway bearing prototype.

### 2.1. Experiment

The primary objective of the experiment was to verify bearing stiffness and capacity. As rings were made from PLA, the bearing behavior was unknown. The axial stiffness was selected as the best way to verify the prototype. A special fixture was created in order to achieve a rigid connection between the machine and the specimen. The stiffness of such a jig can affect the accurateness of measurements. Therefore, it is crucial to exercise special care and attention when using the jig to ensure accurate and reliable measurements. The underlying concept of the experiment was to measure the reaction and displacement of the machine head. Force was applied through jaws to the upper surface of the fixture while the lower surface of the jig was fully fixed. The bearing was bolted between the upper and lower parts of the jig.

### 2.2. FEA equivalent model

In order to obtain sufficient results of all phenomena occurring in bearing, it is necessary to use a very fine mesh. In terms of computing time, it is impossible

to simulate the entire bearing with nonlinear contacts and fine mesh and obtain useful results. To mitigate this problem, the equivalent model of slewing bearing is developed, where nonlinear contacts between components are replaced by nonlinear springs with proper stiffness and rigid beam elements (balls as rolling elements). In the case of 4-point wire raceway bearing, each set of contact between the *ball-wire* is replaced by spring and beam elements, whereas beam elements are connected to a ring on the area corresponding to force distribution in contact pair *wire-ring*. The number of springs and beam element sets corresponds to the number of rolling elements. The ring was modeled by solid elements. The concept is shown in Fig. 3. The length of a single spring is related to the difference between ball's radius and raceway's radius. The initial angle between spring is equal to the corresponding angle between contact points in the bearing.

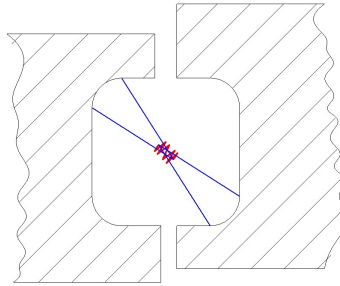


FIG. 3. The concept of the FEA equivalent model (red color – spring elements, blue color – rigid beam elements) shown only for two contact pairs.

To obtain nonlinear spring stiffness, it is necessary to simulate the behavior of contact pair *ball-wire*, as the stiffness of the ring is included in the model by modeling the contact pair as solid elements. An example of stiffness characteristic used in the equivalent model is presented in Fig. 4. Nonlinearity caused by Hertz stress phenomena can be included in the FEA model using a very fine mesh in the contact area. An additional benefit of the equivalent model is the possibility to include bearing preload or clearance by modifying the stiffness characteristics. The stiffness of contact pair *ball-wire* can be calculated in a detailed FEA simulation of a single rolling element and the corresponding length of wire.

To prevent the rotation of the set of springs, additional boundary conditions should be applied to center points, such as angular displacement of center points, according to the cylindrical coordinate system corresponding to the specific bearing design. Beam elements connecting springs and rings should be only responsible for radial and axial movement in the same cylindrical coordinate system.

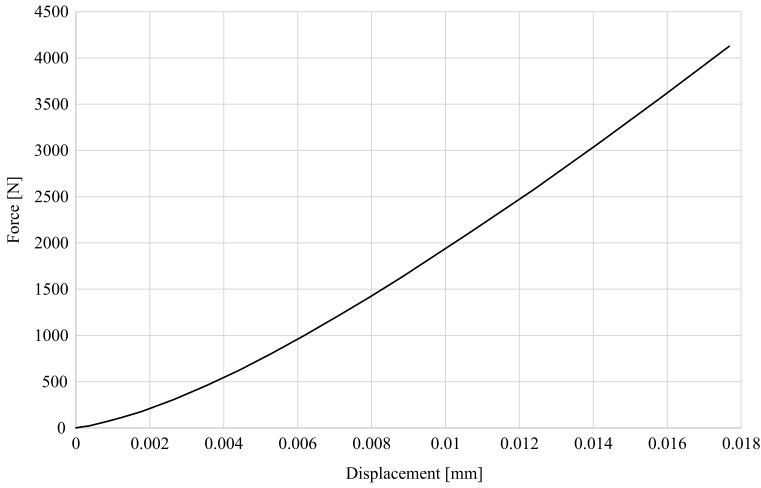


FIG. 4. Nonlinear spring stiffness used in the FEA equivalent model.

Material properties used in both simulations of the contact pair *ball-wire* and the equivalent model are presented in Table 2. All calculations were done in the elastic range of material.

**Table 2.** Material properties used in simulations.

Component	Material	$E$ [GPa]	$\nu$ [-]
Ball	100Cr6	200	0.3
Wire	54SiCr6	200	0.3
Ring	PLA	3.3	0.35
Jig	S235	200	0.3

The FEA equivalent model of the entire wire raceway bearing is presented in Fig. 7.

The model consists of the following components (looking from top to bottom): the upper part of the test jig, the internal ring, the external ring and the lower part of the test jig.

All rolling elements in the simplified model are represented by the set of nonlinear springs and rigid beam elements, as discussed in the previous section. Rings were split into segments in order to obtain a proper contact area between beam elements and rings. Additionally, the test jig was added to the simulation.

In the simulation, the force was applied to the upper surface of the test jig, and the lower part of the test jig was fully fixed (3 DOF). Between the upper part of the test jig and the internal ring, frictional contact was used. The same was applied to the lower part of the test jig and the bottom surface of the

external ring. Each central point of each set of springs and beam elements was fixed in a cylindrical coordinate system, angular displacement ( $\theta$ ) was fixed and rotation R and Z were also fixed. Boundary conditions are presented in Figs. 5 and 6.

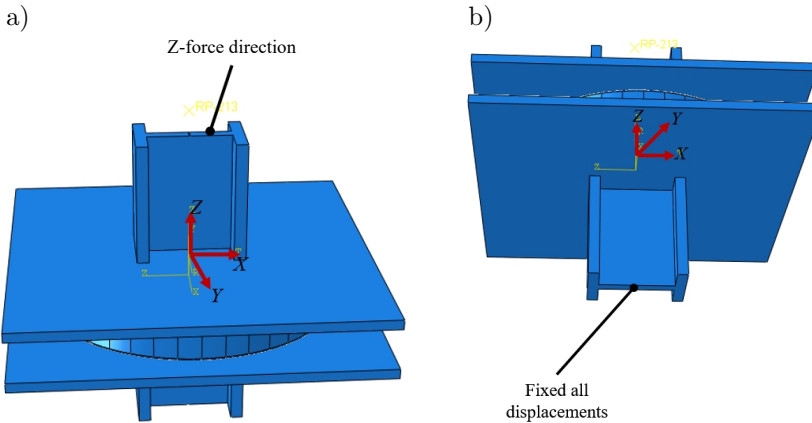


FIG. 5. Boundary conditions used in FEA: a) the upper part of the test jig, b) the bottom part of the test jig.

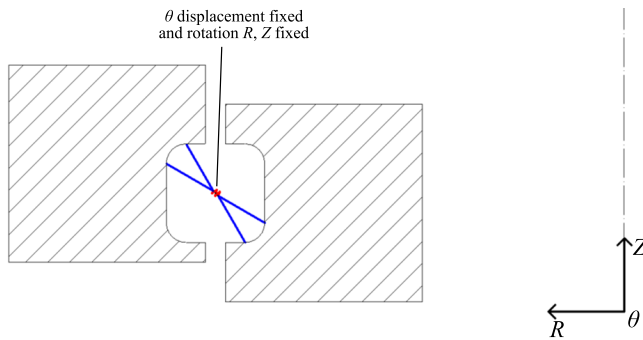


FIG. 6. Boundary conditions for sets of spring and beam elements (only 2 spring and beam elements were presented for clarity).

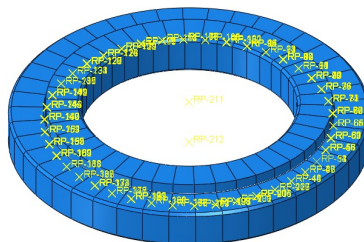


FIG. 7. An example of the FEA equivalent model of wire raceway bearing.

The main advantages of the equivalent model are

- Short calculation time due to the absence of nonlinear contacts.
- Ability to use various loads, such as axial force, radial force and tilting moment.
- Force distribution in every rolling element.
- Ability to include support stiffness, which affects force distribution in rolling elements.
- Preload or clearance can be added and its influence can be analyzed.
- Rings stiffness is included in the simulation, unlike in analytical calculations, where rings are treated as rigid elements.

### 3. RESULTS AND DISCUSSION

The experiment was performed on the universal testing machine (Manufacturer: MTS, model: 318). The prototype was mounted in the machine by jigs and machine jaws. Force was applied to the upper fixing, while the bottom part was fully fixed in the machine jaws. A simple axial compression test was performed, and force and deflection were measured. The prototype of the 3D printed wire raceway bearing mounted in the jig and an example of the FEA equivalent model are presented in Fig. 8.

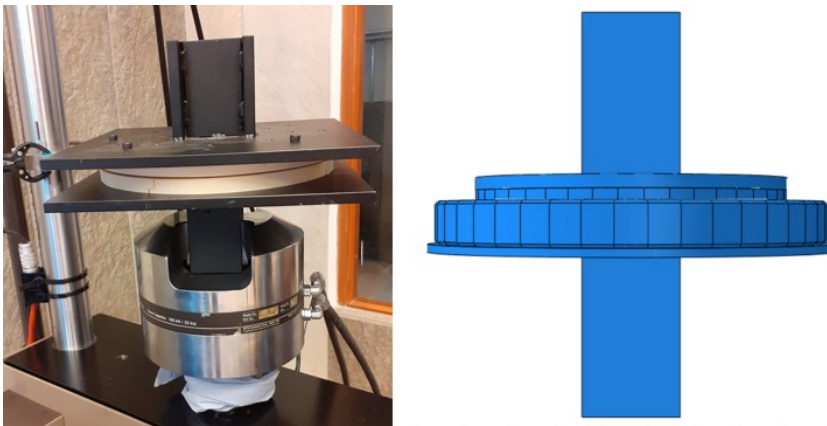


FIG. 8. The assembly of the test jig and the prototype of 3D printed wire raceway bearing (left side) and the FEA equivalent model with the test jig used in the simulation (right side).

The results are presented in Fig. 9. The equivalent model reflected nonlinear bearing characteristics. Maximum force was equal to 50 kN with deflection equal to 5 mm. Deflection, in that case, limits the bearing usage, as it reaches a significant value, which can greatly affect the machine's stiffness. Moreover,

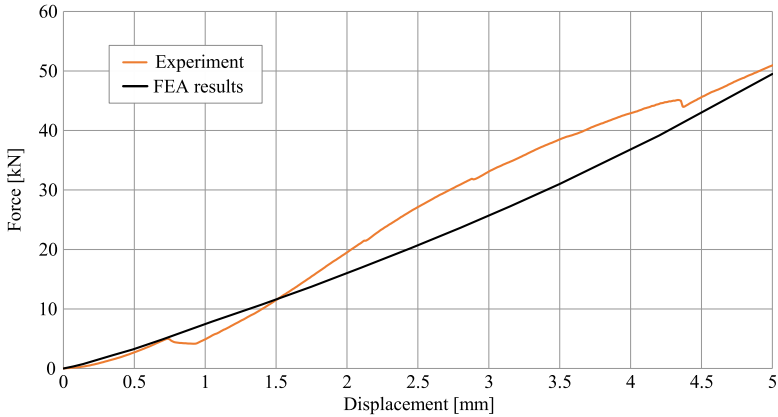


FIG. 9. Comparison of experiment results and FEA simulation results.

the correlation is not that good between the force value of 10 kN to 40 kN. This may be an effect of plastic deformation of the bearing rings as they have much lower mechanical strength than the balls and wire raceway, and also, jig stiffness may affect this range. According to the manufacturer, the capacity of this set of wire raceways bearing with aluminum rings is equal to 117 kN [1].

The first main discrepancy between the experiment and the model can be noticed for the displacement equal to 0.75 mm, which can result from the wire twisting effect [13, 14]. Another potential explanation is plastic deformation on some length of the ring, as 3D printing is not the most accurate method, and the contact surface between *wires-rings* was not equal on the entire circumference.

For higher loads (the discrepancy between the FEA model and the experiment starting from 20 kN), the observed discrepancy can be explained by the stiffness of the test jig and further plastic deformation of PLA rings, resulting in damage to the ring close to a displacement of 4.5 mm.

Due to the fact that the deflection exceeded the feasible range, it was decided to limit the deflection to 0.7 mm. In this range, the correlation between the experiment and FEA equivalent model is still satisfactory. Details are presented in Fig. 10, and the maximum force is equal to 5 kN.

This experiment proves that 3D printing rings can be used in wire raceway bearings but with low capacity. It is worth mentioning that capacity can be satisfactory to many applications, while price and weight are much lower. Moreover, the experiment showed a good correlation for results obtained from the FEA equivalent model, as the bearing behavior was properly reflected in the simulations.

Ball load ( $p_w$ ) is one of the most common ways to calculate force distribution per each rolling element. In the FEA equivalent model, the force can be calcu-

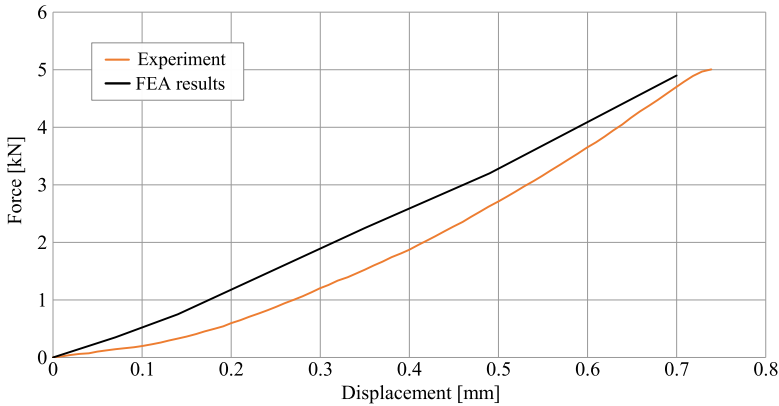


FIG. 10. Comparison of experiment results and FEA simulation results in the range of 0 to 0.7 mm.

lated as the force reaction of a nonlinear spring corresponding to the proper contact pair. Ball load can be calculated by the following formula:

$$(3.1) \quad p_w = \frac{F}{d^2},$$

where  $F$  is the force per ball, and  $d$  is the ball's diameter.

For displacement of 0.7 mm, force value of 5 kN  $p_w$  is equal to 1.3 MPa. For classical slewing bearing, this is low value. However, the ring's material limits the maximum force in this case.

After validating the method, further theoretical calculations were performed to assess the 3D-printed bearing behavior. In the next step, the FEA equivalent model was loaded with combined load (axial force and tilting moment). Two equivalent models were used, first with PLA rings, and second with aluminum rings. The behavior of both bearings was compared, the force distribution in the rolling elements was measured and the rolling elements' angle change was examined.

Additionally, analytical calculations were performed and checked against the FEA equivalent model. As an analytical method, the Ohnrich approach was used to calculate the force distribution in the rolling elements of the bearing [2, 3]. Load values are shown in Table 3. Simulations were conducted similarly to the

**Table 3.** Loads used in load combination 1.

No of load combinations	Load type	Aluminum rings	PLA rings
1	Axial force [kN]	15	15
	Tilting moment [kNm]	0.6	0.6

previous ones; however, the jigs were removed and the lower ring was fixed, while the load was applied to the upper ring.

The results for load combination 1 (Fig. 11) are presented as charts showing the ball load distribution for every rolling element in the contact pairs between *ball-wire raceway*. Moreover, these charts include the results for PLA bearings, aluminum bearings and the analytical results obtained from the Ohnrich method. For the Ohnrich method, with that type of load combination, it is assumed that only two contact pairs carry the load. The ball load for the Ohnrich method achieves the highest value among all calculations, with a maximum value equal to 10.3 MPa for the ball corresponding to 180°. Balls opposite to the maximum ball load have the lowest load, equal to 1.8 MPa. The bearing with aluminum rings has the highest ball load equal to 8.8 MPa and the lowest equal to 4 MPa. The maximum load in the bearing with PLA rings is the lowest among all calculations, with a value equal to 8.2 MPa. It means that the ring stiffness related to the material affects the force distribution in the rolling elements. The minimum ball load for the bearing with PLA rings is equal to 3 MPa.

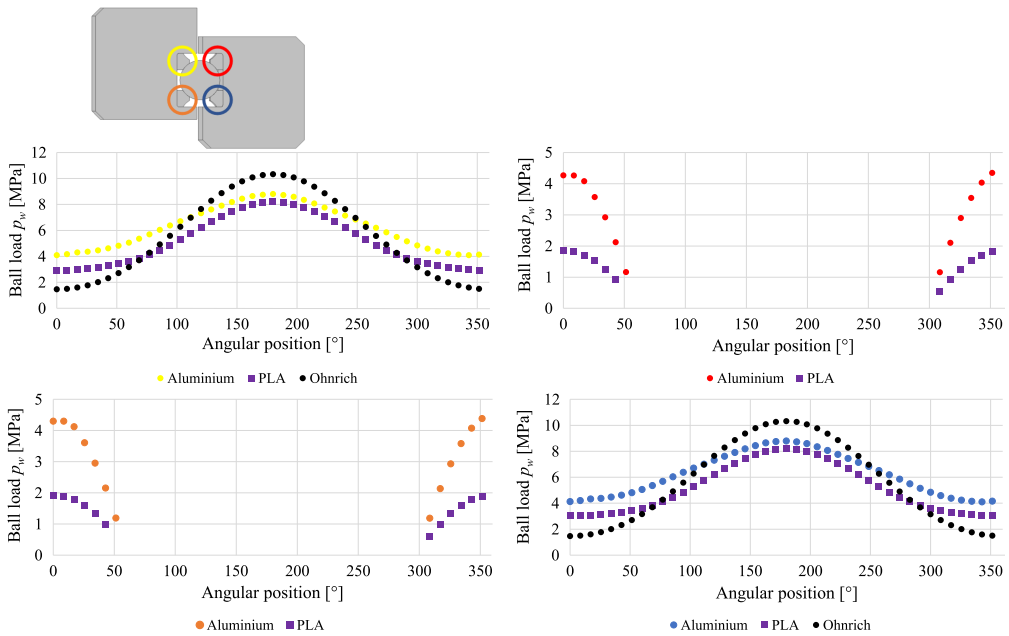


FIG. 11. Comparison of ball load for every contact pair in wire raceway bearing.

For non-main contact pairs (Fig. 9 – chart’s lower left and upper right), both aluminum and PLA bearings transfer some load, whereas aluminum rings tend to transfer two times more than PLA rings (for balls with an angular position

equal to  $0^\circ$ ). For balls with the angular position from  $50^\circ$  to  $310^\circ$ , the contact pairs do not transfer the load.

Both equivalent and analytical models correctly reflect the force distribution in a qualitative manner with proper gradual decreasing of force values.

Percentage differences in the Ohnrich method for the aluminum and PLA bearings are in Table 4.

**Table 4.** Comparison between maximum ball loads in the Ohnrich method.

No of load combinations	Aluminum rings [%]	PLA rings [%]
1	15	20

According to the results, the Ohnrich method may overestimate the maximum ball load and underestimate the minimum ball load. This method also does not provide results for non-main contacts pair. Material affects force distribution, especially for non-main contact pairs. Moreover, it also affects the maximum and minimum values of the ball load. This relation depends on the material, and the aluminum rings have a higher maximum ball load than the PLA rings. At this stage, a material with a higher Young’s modulus value is recommended for bearing rings. The composite with short fibers can be a good choice, as it combines a high Young’s modulus and low density.

The FEA equivalent model allows calculating the contact angle for all contact pairs. Results are presented in Fig. 12, as a contact angle for load combi-

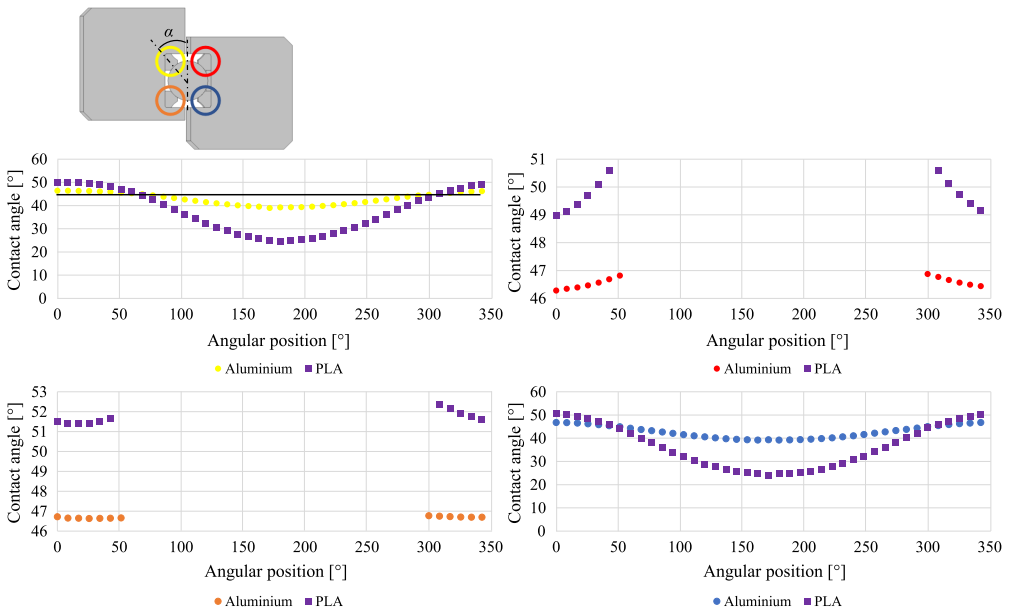


**FIG. 12.** Comparison of contact angle for every contact pair in wire raceway bearing.

nation 1 for every ball. The initial value for this type of the bearing is equal to  $45^\circ$ . The greatest change in contact angle appears for the maximum loaded ball for both cases (aluminum and PLA). The maximum angle for the aluminum rings in loaded contact pairs is equal to  $46.8^\circ$  (balls with an angular position  $0^\circ$ ), while the minimum contact angle is equal to  $39.3^\circ$ . The rigidity of aluminum rings helps to reduce contact angle changes. For non-loaded contact pairs, the maximum and minimum values are equal to  $47^\circ$  and  $46.5^\circ$ , respectively.

PLA rings show significant changes in the contact angle, with a minimum value equal to  $24.7^\circ$  and a maximum value of  $50^\circ$ . Even for non-carrying contact pairs, the contact angle values are still high, ranging from  $49^\circ$  to  $51.8^\circ$ . Due to the lower stiffness of the PLA rings, the forces in the rolling elements may differ significantly due to changes in the contact angle, where force components can differ, whereas the ideal case should be the same.

#### 4. SUMMARY

A study and experiment showed that it is possible to use 3D-printing rings made from PLA in wire raceway bearings. The prototype bearing withstands a load of 50 kN. However, the deflection is significant (5 mm) limiting bearing usage. For lower values of deflection (corresponding to 0.7 mm), the force reaction is equal to 5 kN. This value seems low for slewing and wire raceway bearings; however, it may be satisfactory in some industries such as robotics, where low mass and low inertia are more important.

The main advantages of 3D-printed rings are:

- With lower weight and inertia of bearing, the prototype weight was equal to 1.4 kg, while the aluminum type was 1.7 times heavier. The rings were solid and no shape optimizing algorithm was used for the rings.
- 3D printing offers ease of manufacturing as it eliminates the need for expensive, large-size machining centers. Moreover, 3D printing enables the production of more complicated shapes that may reduce the weight and increase bearing stiffness to meet specific design needs.

The FEA equivalent model concept demonstrated a strong correlation with the experiment, as it accurately reproduced the nonlinear force and deflection characteristics of the prototype. Moreover, the equivalent model is able to simulate bearing and supporting structure, and results are delivered in a fast manner. The method allows using various materials for rings, and in this article, aluminum and PLA were investigated. Additionally, as a result, various outputs can be requested, such as the ball load of each contact pair and contact angle. Aluminum rings have a higher stiffness than PLA rings, which results in

a smaller contact angle change (for maximally loaded balls equal to  $39.3^\circ$  and  $24.7^\circ$ , respectively).

Another validation of the FEA equivalent model was done, by calculating the ball load according to the analytical method. Compared to an analytical method such as the Ohnrich method, the FEA equivalent results have a lower value of ball load for the maximally loaded ball. For minimally loaded balls, values of ball load tend to be higher in the FEA equivalent model than in the Ohnrich method. The distribution of force is similar in each case, which confirms the validity of the FEA model. For aluminum rings, the difference between the analytical method and FEA for maximum ball load is equal to 15%, while for PLA rings, it is equal to 20%.

Due to the higher stiffness of aluminum rings, the ball load in the bearing is higher than in the bearing with PLA rings for all rolling elements.

It was concluded that ring stiffness is critical; hence, further studies on materials are necessary. Ideal material should combine low density and high Young's modulus, and plastics with short fibers seem a good choice, as they can be 3D printed.

## REFERENCES

1. Franke GmbH, *Technical information on wire race bearings*, 2020.
2. SMOLNICKI T., *Large-diameter rolling bearings. Global and local problems* [in Polish: *Wielkogabarytowe toczne węzły obrotowe. Zagadnienia globalne i lokalne*], Oficyna Wydawnicza Politechniki Wrocławskiej, Wrocław 2013.
3. SMOLNICKI T., *Physical aspects of coherence of large-diameter rolling bearings and deformable support structures* [in Polish: *Fizyczne aspekty koherencji wielkogabarytowych łożysk tocznych i odkształcalnych konstrukcji wsporczych*], Oficyna Wydawnicza Politechniki Wrocławskiej, Wrocław 2002.
4. KANIA L., KRYNKE M., MAZANEK E., A catalog capacity of slewing bearings, *Mechanism and Machine Theory*, **58**: 29–45, 2012, doi: 10.1016/j.mechmachtheory.2012.07.012.
5. GLODEŽ S., POTOČNIK R., FLAŠKER J., Computational model for calculation of static capacity and lifetime of large slewing bearing's raceway, *Mechanism and Machine Theory*, **47**: 16–30, 2012, doi: 10.1016/j.mechmachtheory.2011.08.010.
6. POTOČNIK R., GÖNCZ P., FLAŠKER J., GLODEŽ S., Fatigue life of double row slewing ball bearing with irregular geometry, *Procedia Engineering*, **2**(1): 1877–1886, 2010, doi: 10.1016/j.proeng.2010.03.202.
7. DUVAL R., BENNEBACH M., BLASIAK J., GUELBI A., Modeling fatigue behaviour of slewing rings in crane structures. Identification of influencing parameters on local stresses and fatigue damage calculations, *Procedia Engineering*, **213**: 323–334, 2018, doi: 10.1016/j.proeng.2018.02.033.
8. HE P., HONG R., WANG H., LU C., Fatigue life analysis of slewing bearings in wind turbines, *International Journal of Fatigue*, **111**: 233–242, 2018, doi: 10.1016/j.ijfatigue.2018.02.024.

9. SMOLNICKI T., HARNATKIEWICZ P., STAŃCO M., Degradation of a geared bearing of a stacker, *Archives of Civil and Mechanical Engineering*, **10**(2): 131–139, 2010, doi: 10.1016/S1644-9665(12)60055-7.
10. KANIA L., PYTLARZ R., ŚPIEWAK S., Modification of the raceway profile of a single-row ball slewing bearing, *Mechanism and Machine Theory*, **128**: 1–15, 2018, doi: 10.1016/j.mechmachtheory.2018.05.009.
11. GUNDUZ A., SINGS R., Stiffness matrix formulation for double row angular contact ball bearing: Analytical development and validation, *Journal of Sound and Vibration*, **332**(22): 5898–5916, 2013, doi: 10.1016/j.jsv.2013.04.049.
12. HE P., DING Y., WANG Y., LI F., LIU W., WANG H., A new analysis method for the carrying capacity of three-row roller slewing bearing, *Mechanika*, **28**(4): 266–272, 2022, doi: 10.5755/j02.mech.29914.
13. MARTÍN I., HERAS I., CORIA I., ABASOLO M., AGUIRREBEITIA J., Structural modeling of crossed roller wire race bearings: Analytical submodel for the roller-wire-ring set, *Tribology International*, **151**: 106420, 2020, doi: 10.1016/j.triboint.2020.106420.
14. MARTÍN I., HERAS I., AGUIRREBEITIA J., MACARENO L.M., Influence of the geometrical design on ball and crossed roller wire race bearing behaviour under axial load, *Tribology International*, **156**: 106817, 2021, doi: 10.1016/j.triboint.2020.106817.
15. MARTÍN I., HERAS I., AGUIRREBEITIA J., ABASOLO M., CORIA I., Static structural behaviour of wire bearings under axial load: Comparison with conventional bearings and study of design and operational parameters, *Mechanism and Machine Theory*, **132**: 98–107, 2019, doi: 10.1016/j.mechmachtheory.2018.10.016.
16. MARTÍN I., AGUIRREBEITIA J., HERAS I., ABASOLO M., Efficient finite element modeling of crossed roller wire race slewing bearings, *Tribology International*, **161**: 107098, 2021, doi: 10.1016/j.triboint.2021.107098.
17. GUNIA D., SMOLNICKI T., The influence of the geometrical parameters for stress distribution in wire raceway slewing bearing, *Archive of Mechanical Engineering*, **64**(3): 315–326, 2017, doi: 10.1515/meceng-2017-0019.

*Received March 1, 2023; accepted version July 14, 2023.*



Copyright © 2023 The Author(s).

This is an open-access article distributed under the terms of the Creative Commons Attribution-ShareAlike 4.0 International (CC BY-SA 4.0 <https://creativecommons.org/licenses/by-sa/4.0/>) which permits use, distribution, and reproduction in any medium, provided that the article is properly cited. In any case of remix, adapt, or build upon the material, the modified material must be licensed under identical terms.